Medium-spin states in ^{135}Cs

N. Fotiades,[1,*] J. A. Cizewski,[2] K. Higashiyama,[3] N. Yoshinaga,[4] E. Teruya,[4] R. Krücken,[5] R. M. Clark,[6] P. Fallon,[6] I. Y. Lee,[6] A. O. Macchiavelli,[6] and W. Younes[7]

[1]*Los Alamos National Laboratory, Los Alamos, New Mexico 87545, USA*
[2]*Department of Physics and Astronomy, Rutgers University, New Brunswick, New Jersey 08903, USA*
[3]*Department of Physics, Chiba Institute of Technology, Narashino, Chiba 275-0023, Japan*
[4]*Department of Physics, Saitama University, Saitama City 338-8570, Japan*
[5]*TRIUMF, Vancouver, V6T 2A3, Canada*
[6]*Nuclear Science Division, Lawrence Berkeley National Laboratory, Berkeley, California 94720, USA*
[7]*Lawrence Livermore National Laboratory, Livermore, California 94550, USA*

(Received 12 August 2013; revised manuscript received 1 November 2013; published 12 December 2013)

Limited information is currently known on medium- and higher-spin states for ^{135}Cs, a neutron-rich nucleus amenable to shell-model calculations due to its proximity to the shell closures in ^{132}Sn. In order to extend the level structure of ^{135}Cs to higher excitations, this nucleus was studied via prompt γ-ray spectroscopy of fragments following the fission of the compound nucleus ^{226}Th formed in the ^{18}O (91 MeV) + ^{208}Pb fusion-fission reaction. Medium-spin states up to spin (23/2) and ~3.3 MeV excitation energy have been established. The observed states were compared with those in the neighboring $N = 82$ ^{137}Cs nucleus, as well as with states in the neighboring $N = 80$ isotones. The coupling of the odd proton occupying the $g_{7/2}$ orbital to the yrast states in the ^{134}Xe and ^{136}Ba cores could account for the lower excited states of ^{135}Cs. The experimental results are compared with predictions from shell-model calculations.

DOI: 10.1103/PhysRevC.88.064315 PACS number(s): 21.60.Cs, 23.20.Lv, 27.60.+j

I. INTRODUCTION

The study of medium- and higher-spin states in isotopes near the $N = 82$ closed shell with a few protons beyond the $Z = 50$ closed shell is of interest in order to enrich our knowledge in the vicinity of these magic numbers and to test nuclear shell-model calculations that make use of effective interactions. In particular, the level structure of the $^{135}_{55}Cs_{80}$ isotope with only two neutron holes in the $N = 82$ shell is very interesting because of the relatively limited number of single-particle configurations available for the construction of medium- and higher-spin states.

^{135}Cs is also important in applications of nuclear physics. Recently, ^{135}Cs has been identified [1] as an important branch point in the nucleosynthesis in the slow neutron capture (s) process [2,3]. Moreover, since it is a very long-lived isotope (2.3×10^6 years) and it is produced as a fragment in the fissioning of actinides, it is also of special interest for studies and projects that handle the transmutation of nuclear fuel (see, for instance, Ref. [4]).

The underlying nuclear structure configurations in ^{135}Cs are expected to involve the proton $g_{7/2}$ and $d_{5/2}$ orbitals and the neutron $s_{1/2}$, $d_{3/2}$, and $h_{11/2}$ orbitals at lower excitations, while the proton $h_{11/2}$ orbital can play an important role at higher excitations. Indeed, in the neighboring $^{137}Cs_{82}$ [5–7] the closure of the neutron shell allows a straightforward interpretation of the states using only proton configurations up to 4 MeV excitation energy. The proton $h_{11/2}$ orbital in ^{137}Cs comes into play at ~3.3 MeV excitation energy. The situation in ^{135}Cs is expected to be similar with a few extra excitations possible (for similar excitation energies) due to the two neutron holes occupying the $s_{1/2}$, $d_{3/2}$, and $h_{11/2}$ orbitals.

The existing information on the low-lying levels for ^{135}Cs [8] was obtained mostly in β-decay measurements. A $19/2^-$ isomer has also been observed [8,9] in ^{135}Cs at 1633-keV excitation energy and represents the lowest level that includes a neutron hole in the $h_{11/2}$ orbital. For the positive-parity states, the $11/2^+$ state at 786.8-keV excitation energy is the highest-spin positive-parity state known in this nucleus and deexcites only towards the $7/2^+$ ground state with a strong $E2$ transition. ^{135}Cs has never been studied in a fusion evaporation reaction [8] mainly due to the limited stable target-projectile options that can populate this isotope as an evaporation residue in heavy-ion fusion reactions. Hence, the existing information on medium- and higher-spin states for ^{135}Cs is very limited. An alternative way to study this neutron-rich nucleus is the prompt γ-ray spectroscopy of fission fragments following fusion-fission reactions of much heavier nuclei. Due to the proximity to the line of stability, ^{135}Cs is expected to be populated as a fission fragment in such reactions. In the present work excited states in ^{135}Cs, up to 3.3 MeV in energy, have been identified by prompt γ-ray spectroscopy of fragments following fission in a heavy-ion-induced reaction.

II. EXPERIMENT

The 88-Inch Cyclotron Facility at Lawrence Berkeley National Laboratory was used to populate a ^{226}Th compound nucleus in the ^{18}O + ^{208}Pb reaction at 91 MeV. The target was 45 mg/cm^2 in areal density. The Gammasphere array was used for subsequent γ-ray spectroscopy. Gammasphere comprised 100 Compton-suppressed large volume HPGe detectors. About 2.5×10^9 fourfold γ-ray coincidences were collected

*fotia@lanl.gov

in the experiment. A symmetrized, three-dimensional cube was constructed to investigate the prompt-time coincidence relationships between the γ rays. ^{135}Cs was one of the several fission fragments populated. The data from this experiment have been used for γ-ray spectroscopy of other fission fragments in Refs. [10–12].

III. EXPERIMENTAL RESULTS

The level scheme of ^{135}Cs deduced in the present work is shown in Fig. 1. The intensities of the transitions relative to the previously known [8] 786.8-keV $11/2^+ \rightarrow 7/2^+$ transition, are also displayed in Fig. 1. The information on the transitions in Fig. 1 is summarized in Table I. In principle, one could start building the level scheme above the 786.8-keV transition by placing a single gate on this transition in the data. However, generally in such experiments more than 100 fragments are populated at high spin, producing several thousands of transitions, which have to be sorted out, thus rendering single-gated spectra useless in the majority of cases. The selection of one particular fragment needs at least two energy conditions, implying that at least two γ rays have to be known. Fortunately, the identification of transitions in one fragment in such experiments can be based on the fact that prompt

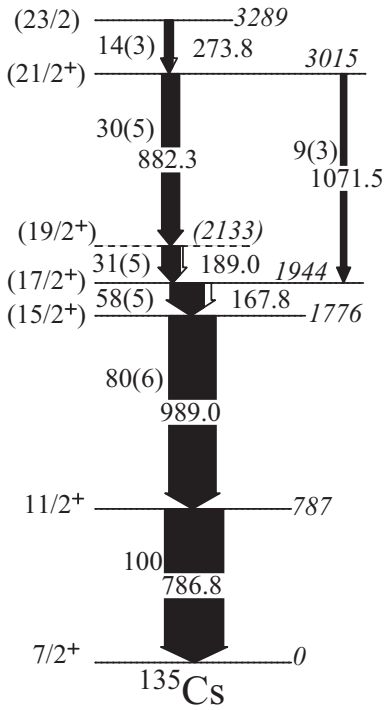

FIG. 1. Level scheme assigned to ^{135}Cs in the present work. Transition and excitation energies are given in keV. The intensities of the transitions are a percentage of the intensity of the 786.8-keV transition. The widths of the arrows are representative of the relative intensity of the transitions. The white part of the arrows is representative of the relative-intensity correction due to internal conversion assuming stretched transitions; this correction is not included in the quoted relative intensities. The intensities of the 189.0- and 882.3-keV transitions are equal within uncertainties; hence, their ordering is tentative.

TABLE I. Energies, intensities, excitation energy of initial level, and spin-parity assignments of initial and final levels for all transitions of ^{135}Cs discussed in the present work.

E_γ (keV)	Intensity (%)	E_i (keV)	$J_i^\pi \rightarrow J_f^\pi$
167.8(5)	58(5)	1944(1)	$(\frac{17}{2}^+) \rightarrow (\frac{15}{2}^+)$
189.0(5)	31(5)	2133(1)[a]	$(\frac{19}{2}^+) \rightarrow (\frac{17}{2}^+)$
273.8(6)	14(3)	3289(2)	$(\frac{23}{2}) \rightarrow (\frac{21}{2}^+)$
786.8(4)	≡100	786.8(4)	$\frac{11}{2}^+ \rightarrow \frac{7}{2}^+$
882.3(7)	30(5)	3015(1)	$(\frac{21}{2}^+) \rightarrow (\frac{19}{2}^+)$
989.0(5)	80(6)	1775.8(9)	$(\frac{15}{2}^+) \rightarrow \frac{11}{2}^+$
1071.5(9)	9(3)	3015(1)	$(\frac{21}{2}^+) \rightarrow (\frac{17}{2}^+)$

[a]See text for possible reordering of 189.0- and 882.3-keV transitions.

γ rays emitted by the complementary fragments are detected in coincidence. In the present case, the previously known 786.8-keV transition was first identified in double gates set on transitions of the ^{85}Br [10,13,14] complementary fragment. ^{85}Br, an odd-even nucleus, is the six-neutron channel with respect to the ^{226}Th compound nucleus and together with the five-neutron channel populating ^{86}Br, an odd-odd nucleus, are the most intensive Br-Cs channels; gates that involve transitions from the odd-even complementary fragment are preferred because they are expected to have better statistics compared to the increased fragmentation of γ-ray strength in the odd-odd nucleus. The 989.0-keV transition was then identified in double gates set on the 786.8-keV transition of ^{135}Cs and transitions belonging to the ^{85}Br complementary fragment, as shown in the spectrum in Fig. 2. The rest of

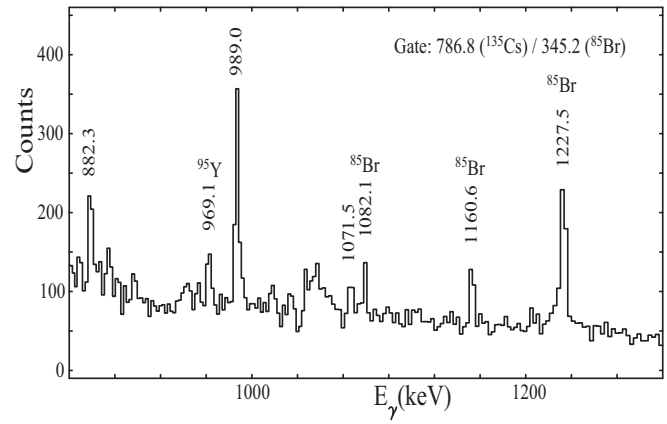

FIG. 2. Background-subtracted γ-ray spectrum double gated on the 786.8-keV transition of ^{135}Cs and on the 345.2-keV transition from the first excited state of the complementary fragment ^{85}Br [13]. The energies of the transitions are in keV. Three transitions assigned to ^{135}Cs in Fig. 1 (882.3, 989.0, and 1071.5 keV) are indicated together with three previously known transitions of ^{85}Br [10,14]. Unlabeled peaks are most likely contaminants, for example the 969.1-keV transition of ^{95}Y [15,16] is indicated, which originates from simultaneous double gating on the 345.6- and 788.0-keV transitions of this nucleus.

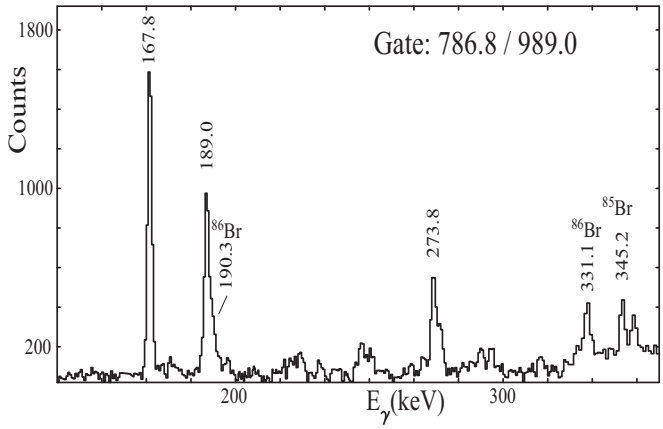

FIG. 3. Background-subtracted γ-ray spectrum double gated on the 786.8- and 989.0-keV transitions assigned to ^{135}Cs and displayed in Fig. 1. The energies of the transitions are in keV. The 345.2-keV transition from the first excited state of the ^{85}Br complementary fragment [13] and two transitions from ^{86}Br [17] are also indicated. Unlabeled peaks are most likely contaminants.

the level scheme in Fig. 1 can then be built based on double gates that include the 786.8- and 989.0-keV transitions. As a corroboration of the assignment, the 989.0-keV transition was also identified in double gates set on the 786.8-keV transition and transitions belonging to the ^{86}Br complementary fragment [17]. The 882.3-, 989.0-, and 1071.5-keV transitions in Fig. 1 can be seen in the spectrum in Fig. 2 and the 167.8-, 189.0-, and 273.8-keV transitions in Fig. 1 can be seen in the spectrum in Fig. 3. The intensities of the 189.0- and 882.3-keV transitions in Fig. 1 are equal within uncertainties after considering the intensity correction due to internal conversion (M1 multipolarities assumed); hence, their ordering in the level scheme should be considered tentative. The ordering selected in Fig. 1 was chosen based on comparison with the neighboring $N = 80$ nuclei as discussed below.

Spin and parity assignments of all new levels reported in this work are difficult to deduce experimentally due to the lack of directional correlation information with respect to the beam for the fission products. For the strongest populated fragments around ^{110}Ru in the present reaction some directional correlation information can be obtained in the way described in Ref. [18]. For weakly populated fission products, such as ^{135}Cs, low statistics for γ-ray directional correlation information prevented such analysis. However, spin and parity assignments have been tentatively suggested based on comparison with the medium-spin structure in the neighboring ^{137}Cs nucleus [5–7] and neighboring isotones ^{133}I [19,20], ^{134}Xe [21], and ^{136}Ba [22–24] (see Fig. 4).

The $19/2^-$ isomer observed in ^{135}Cs at 1633-keV excitation energy [8,9] is at a lower excitation energy compared to the $(19/2^+)$ state in Fig. 1; hence, it is yrast. Consequently, a non-negligible part of the deexcitation of the nucleus is expected to proceed through this isomer after the population of ^{135}Cs as a fission fragment in the present work. No transitions have been previously observed above this isomer. Therefore, the identification of transitions in the present data

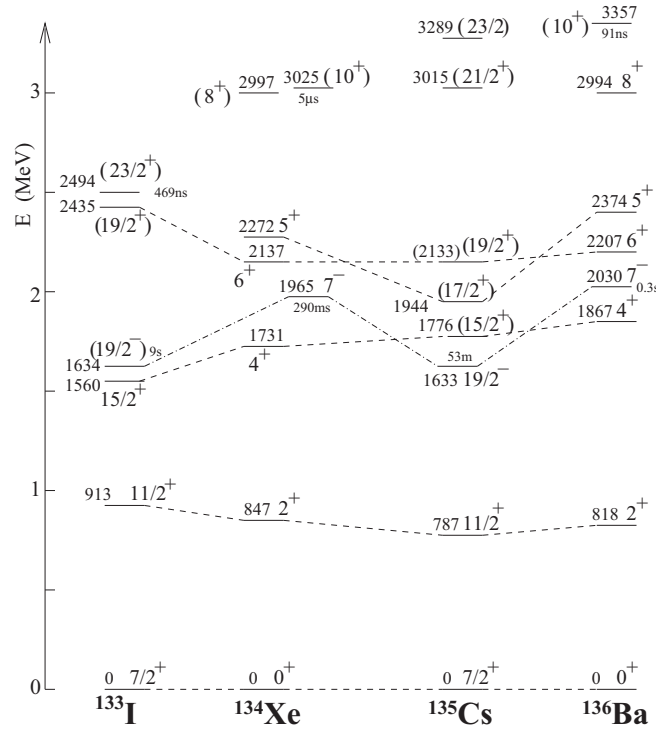

FIG. 4. Medium-spin states assigned to ^{135}Cs in the present work compared with excited states in the isotones ^{133}I [19,20], ^{134}Xe [21], and ^{136}Ba [22,23]. The previously known $19/2^-$ isomer of ^{135}Cs [8] is also included for discussion purposes.

above the $19/2^-$ isomer has to be based entirely on the complementary fission fragment technique, which requires the observation of such transitions in double gates of previously known transitions in at least two different complementary fission fragments. Poor statistics in double gates involving the odd-odd ^{86}Br [17,25] complementary fragment and the lack of previously known suitable transitions on which to place double gates in the complementary fragment of ^{87}Br [26,27] (the five- and four-neutron channels, respectively, with respect to the ^{226}Th compound nucleus) prohibited the observation of any transitions feeding the $19/2^-$ isomer of ^{135}Cs in the present work.

IV. DISCUSSION

All the states observed in ^{135}Cs in the present experiment up to the 3015-keV level are tentatively assigned as positive-parity states in Fig. 1. The lowest negative-parity state known in ^{135}Cs is the $19/2^-$ isomer [8,9] and has been interpreted using three-particle configurations that contain one neutron hole in the $h_{11/2}$ orbital [9]. The lowest excited state with a proton in the $h_{11/2}$ orbital is expected to be at $\sim$2 MeV in energy; no experimental evidence for such a state has been observed. At higher excitation energies, several other negative parity states are expected; such states have been observed in the neighboring ^{137}Cs [5–7]. The negative-parity states populated in the present experiment are expected to deexcite primarily towards the $19/2^-$ isomer. As discussed

in the previous section, these states were not observed in the present work.

In Fig. 4 the states of ^{135}Cs observed in the present work are compared to the states in the $Z = 54, 56$ cores of ^{134}Xe [21] and ^{136}Ba [22–24], as well as with the states in the isotone ^{133}I [19,20]. A one-to-one correspondence is possible between the states connected by dashed lines in Fig. 4 up to ∼2 MeV excitation energy based on the coupling of the odd proton in the $g_{7/2}$ orbital to the configurations of the states in the cores. The same is true also for the previously known $19/2^-$ isomer for which the corresponding 7^- isomers in the cores are included in the figure, although the coupling is not stretched in this case. At higher excitations, it is possible that the 3015- and/or 3289-keV levels originate from the same coupling to the 8^+ states of the cores. A second isomer with spin-parity assignment (10^+) is known in both ^{134}Xe and ^{136}Ba and was included in Fig. 4. The configuration of this high-spin isomer involves two neutron holes in the $h_{11/2}$ orbital. Similar 10^+ isomers have been observed in all of the neighboring even-mass $N = 80$ isotones [28,29] while in the lighter odd-mass ^{131}Sb [30] and ^{133}I [19,20] $(23/2^+)$ isomers are known. The 3289-keV level could be the corresponding $(23/2^+)$ state in ^{135}Cs. As mentioned above, the ordering of the 189.0- and 882.3-keV transitions in Fig. 1 is tentative due to their equal intensities, within uncertainties. The ordering proposed in Fig. 1 was chosen because it renders the $(19/2^+)$ level at an excitation energy of 2133 keV, which lies very close to the 6^+ states of the cores, as seen in Fig. 4. A reordering of the 189.0- and 882.3-keV transitions in Fig. 1 that would shift the $(19/2^+)$ level to 2826-keV excitation energy can not be ruled out. As a consequence, such a 2826-keV level would not be suitable for a one-to-one correspondence to the 6^+ states of the cores, which lie at lower excitation energies.

Shell-model calculations for ^{135}Cs have been reported in the past [31–34] but the predictions are limited to lower-spin states (up to spin $11/2$) and, hence, cannot be directly compared with the present experimental results. In the present work these predictions were extended to higher spins and excitation energies. The single-particle valence space consists of the five $0g_{7/2}$, $1d_{5/2}$, $1d_{3/2}$, $0h_{11/2}$, and $2s_{1/2}$ orbitals in the major shell between the magic numbers 50 and 82. Adopted single-particle energies are extracted from experimental values of ^{131}Sn and ^{133}Sb, and take the values (in MeV) of $\varepsilon(0g_{7/2}) = 2.434$ (-0.200), $\varepsilon(1d_{5/2}) = 1.655$ (0.962), $\varepsilon(1d_{3/2}) = 0.0$ (2.440), $\varepsilon(0h_{11/2}) = 0.285$ (2.791), $\varepsilon(2s_{1/2}) = 0.332$ (3.000) for neutron holes (proton particles).

The effective shell-model Hamiltonian is written as

$$\hat{H} = \hat{H}_\nu + \hat{H}_\pi + \hat{H}_{\nu\pi}, \qquad (1)$$

where $\hat{H}_\nu$, $\hat{H}_\pi$, and $\hat{H}_{\nu\pi}$ represent the neutron interaction, the proton interaction, and the neutron-proton interaction, respectively. The interaction among like nucleons $\hat{H}_\tau$ ($\tau = \nu$ or π) consists of spherical single-particle energies, a monopole-pairing interaction (*MP*), a quadrupole-pairing interaction (*QP*), a quadrupole-quadrupole interaction (*QQ*), a hexadecapole-hexadecapole (*HH*) interaction, and higher multipole-pairing (*HMP*) interactions with angular momentum $J = 4,\ 6,\ 8,\ 10$. A quadrupole-quadrupole interaction is

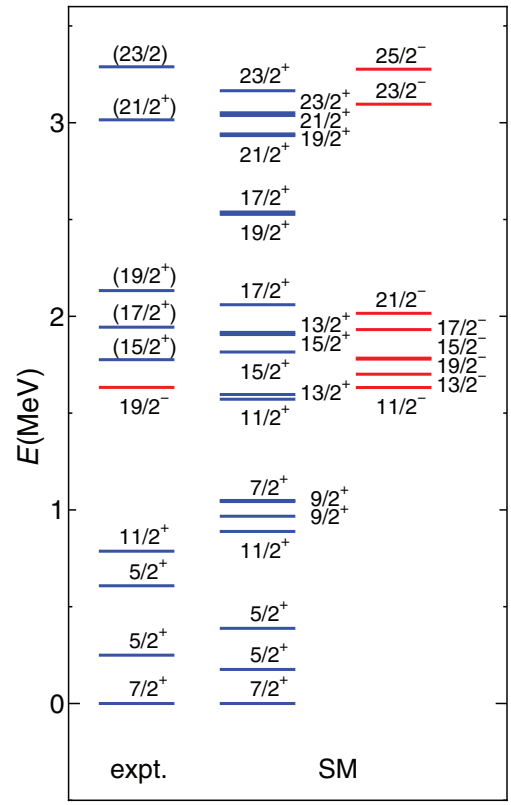

FIG. 5. (Color online) Comparison between the experimental level scheme (expt.) assigned to ^{135}Cs in the present work and previous work [8] with shell model results (SM) for positive-parity states with spins $I \geqslant 5/2$ and negative-parity states with spins $I \geqslant 11/2$.

employed as the neutron-proton interaction. These interactions and their strengths are described in detail in Ref. [35], except for the *HMP* and *HH* interactions, which are defined as the extensions of the *QP* and *QQ* interactions for angular momenta other than two, but no radial dependence (namely r dependence) is assumed. The strengths of the interactions among identical nucleons are adjusted to fit experimental data for singly closed nuclei, and those between neutrons and protons are determined to reproduce the energy levels for open shell nuclei. The determined strengths for ^{135}Cs are $G_{0\nu} = 0.160$, $G_{2\nu} = 0.018$, $\kappa_\nu = 0.010$, $\kappa_{4\nu} = 0.600$, $G_{0\pi} = 0.150$, $G_{2\pi} = 0.010$, $\kappa_\pi = 0.055$, $\kappa_{4\pi} = 0.500$, $G_{4\nu} = G_{4\pi} = 0.200$, $G_{6\nu} = G_{6\pi} = 0.100$, $G_{8\nu} = G_{8\pi} = -6.15$, $G_{10\nu} = G_{10\pi} = -9.50$, and $\kappa_{\nu\pi} = -0.100$ in units of MeV. The results are shown in Fig. 5 and are in reasonable agreement with the experimentally observed medium-spin states reproducing the ordering of these levels. In order to interpret the shell-model results, $B(E2)$ values were calculated for $15/2^+$ states to the first and second $11/2^+$ states, as displayed in Table II. The effective charges are fixed as $e_\nu = -0.75e$ and $e_\pi = +1.75e$ using the prescription $e_\nu = -\delta e$ and $e_\pi = (1 + \delta)e$ so as to reproduce the experimental $B(E2)$ values of the even-even and odd-mass nuclei in this mass region. The neutron effective charge is chosen to be negative, as valence neutrons are treated as holes. From the ratios in Table II it is inferred that the experimentally observed $(15/2^+)$ state corresponds to the $15/2^+_1$ state in the calculation.

TABLE II. Calculated $E2$ transition rates for $15/2^+ \rightarrow 11/2^+$ transitions in ^{135}Cs from the I_i^π state to the I'^π_f state (in units of $e^2\,b^2$) and ratio of these rates.

$I_i^\pi \rightarrow I'^\pi_f$	$B(E2)$	$I_i^\pi \rightarrow I'^\pi_f$	$B(E2)$	$B(E2)$ Ratio
$15/2_1^+ \rightarrow 11/2_1^+$	0.0555	$15/2_1^+ \rightarrow 11/2_2^+$	0.0004	138
$15/2_2^+ \rightarrow 11/2_1^+$	0.0166	$15/2_2^+ \rightarrow 11/2_2^+$	0.02	0.84

V. CONCLUSION

In summary, medium-spin states of ^{135}Cs have been observed following the fission of a hot compound nucleus formed in a fusion-fission reaction. The assignment of the transitions is based on coincidences with a previously known lower-lying transition, as well as with known transitions in the complementary fragments. The observed states can be understood as originating from configurations involving the coupling of the odd proton in the $g_{7/2}$ orbital to the excited states in the $Z = 54, 56$ cores. Shell-model calculations were performed and compare favorably with the observed level scheme. More experimental information, especially firm spin and parity assignments of the states reported here, is needed to confirm the interpretations suggested in the present work.

ACKNOWLEDGMENTS

This work has been supported in part by the U.S. Department of Energy under Contracts No. DE-AC52-06NA25396 (LANL), No. DE-AC52-07NA27344 (LLNL), and No. AC03-76SF00098 (LBNL), by the National Science Foundation (Rutgers), and by the Japan Society for the Promotion of Science under grants in aid for scientific research No. 24540251 and No. 25400267.

[1] A. Couture and R. Reifarth, At. Data Nucl. Data Tables **93**, 807 (2007).
[2] F. Käppeler and A. Mengoni, Nucl. Phys. A **777**, 291 (2006).
[3] F. Käppeler, Prog. Nucl. Part. Phys. **43**, 419 (1999).
[4] R. Takashima, S. Hasegawa, K. Nemoto, and K. Kato, Appl. Phys. Lett. **86**, 011501 (2005).
[5] R. Broda *et al.*, Phys. Rev. C **59**, 3071 (1999).
[6] K. Li *et al.*, Phys. Rev. C **75**, 044314 (2007).
[7] E. Browne and J. K. Tuli, Nucl. Data Sheets **108**, 2173 (2007).
[8] B. Singh, A. A. Rodionov, and Y. L. Khazov, Nucl. Data Sheets **109**, 517 (2008).
[9] I. B. Häller and B. Jung, Nucl. Phys. **52**, 524 (1964).
[10] N. Fotiades *et al.*, Phys. Rev. C **71**, 064312 (2005).
[11] N. Fotiades *et al.*, Phys. Rev. C **74**, 034308 (2006).
[12] N. Fotiades *et al.*, Phys. Rev. C **84**, 054310 (2011).
[13] H. Sievers, Nucl. Data Sheets **62**, 271 (1991).
[14] A. Astier *et al.*, Eur. Phys. J. A **30**, 541 (2006).
[15] S. K. Basu, G. Mukherjee, and A. A. Sonzogni, Nucl. Data Sheets **111**, 2555 (2010).
[16] W. Urban *et al.*, Phys. Rev. C **79**, 044304 (2009).
[17] M.-G. Porquet *et al.*, Eur. Phys. J. A **40**, 131 (2009).
[18] D. Patel *et al.*, J. Phys. G: Nucl. Part. Phys. **28**, 649 (2002).
[19] H. Watanabe *et al.*, Phys. Rev. C **79**, 064311 (2009).
[20] Yu. Khazov, A. Rodionov, and F. G. Kondev, Nucl. Data Sheets **112**, 855 (2011).
[21] A. A. Sonzogni, Nucl. Data Sheets **103**, 1 (2004).
[22] J. J. Valiente-Dobón *et al.*, Phys. Rev. C **69**, 024316 (2004).
[23] T. Shizuma *et al.*, Eur. Phys. J. A **20**, 207 (2004).
[24] A. A. Sonzogni, Nucl. Data Sheets **95**, 837 (2002).
[25] B. Singh, Nucl. Data Sheets **94**, 1 (2001).
[26] R. G. Helmer, Nucl. Data Sheets **95**, 543 (2002).
[27] M.-G. Porquet *et al.*, Eur. Phys. J. A **28**, 153 (2006).
[28] B. Singh, Nucl. Data Sheets **93**, 33 (2001).
[29] J. Genevey, J. A. Pinston, C. Foin, M. Rejmund, R. F. Casten, H. Faust, and S. Oberstedt, Phys. Rev. C **63**, 054315 (2001).
[30] J. Genevey, J. A. Pinston, H. Faust, C. Foin, S. Oberstedt, and M. Rejmund, Eur. Phys. J. A **9**, 191 (2000).
[31] L. Y. Jia, H. Zhang, and Y. M. Zhao, Phys. Rev. C **76**, 054305 (2007).
[32] K. Higashiyama and N. Yoshinaga, Phys. Rev. C **83**, 034321 (2011).
[33] R. Okamoto, Prog. Theor. Phys. **58**, 376 (1977).
[34] D. C. Choudhury and J. N. Friedman, Phys. Rev. C **3**, 1619 (1971).
[35] K. Higashiyama, N. Yoshinaga, and K. Tanabe, Phys. Rev. C **65**, 054317 (2002).